Recovering Missing Component Dependence for System Reliability Prediction via Synergy between Physics and Data

Huiru Li[1,2], Xiaoping Du[1]

[1]Department of Mechanical and Energy Engineering, Indiana University - Purdue University Indianapolis, IN, United States

[2]School of Mechanical Engineering, Purdue University, West Lafayette, IN, United States

ABSTRACT

Predicting system reliability is often a core task in systems design. System reliability depends on component reliability and dependence of components. Component reliability can be predicted with a physics-based approach if the associated physical models are available. If the models do not exist, component reliability may be estimated from data. When both types of components coexist, their dependence is often unknown, and the component states are therefore assumed independent by the traditional method, which can result in a large error. This work proposes a new system reliability method to recover the missing component dependence, thereby leading to a more accurate estimate of the joint probability density (PDF) of all the component states. The method works for series systems whose load is shared by its components that may fail due to excessive loading. For components without physical models available, the load data are recorded upon failure, and equivalent physical models are created; the model parameters are estimated by the proposed Bayesian approach. Then models of all component states become available, and the dependence of component states, as well as their joint PDF, can be estimated. Four examples are used to evaluate the proposed method, and the results indicate that the method can produce more

accurate predictions of system reliability than the traditional method that assumes independent component states.

Keywords: Reliability; System; Bayesian method; Uncertainty; Optimization

1. INTRODUCTION

For many system design problems, it is crucial to predict the reliability of the system under design. The reliability prediction can help not only evaluate and select design concepts, but also produce a design that satisfies the reliability requirement. Doing so in the design stage is more effective than addressing any reliability issues after the system is already in operation.

The system designer usually quantifies system reliability by the probability that a system works properly without failures. The reliability may be estimated either by a physics-based approach [1-4] or a statistics-based approach [5, 6]. A physics-based approach predicts the reliability using computational models derived from physics principles, and the computational models are called limit-state functions. On the other hand, a statistics-based approach estimates the reliability using data from fields or experiments.

When the dependence between component states is unknown, the states of components are usually assumed independent. Under this assumption, the system reliability R_s of a series system is given by [6]

$$R_s = \prod_{i=1}^{n} R_i \tag{1}$$

where R_i is the reliability of component i, and n is the number of components. The independence assumption may result in a significant error if component states are strongly dependent [7].

Many statistics-based methods for component reliability are available in reliability engineering [6]. Physics-based methods for component reliability have also been extensively investigated. The most widely used component reliability methods include the First Order Reliability Method (FORM) [8-10], the Second Order Reliability (SORM) [11-13], Monte Carlo simulation (MCS) methods [14, 15], Saddlepoint approximations (SPA) [16-19], and metamodeling methods [20-22].

Physics-based component reliability methods can be easily extended to system reliability analysis when all component limit-state functions are available. In principle, the joint PDF of all the component states can be derived from the limit-state functions by FORM, SORM, SPA, MCS, and other methods [2, 7, 21-24].

If some of the limit-state functions, however, are not available, the joint PDF of all component states will be unknown. For example, if some of the components are outsourced, their limit-state functions are proprietary to the component suppliers and are unknown to the system designer. If the reliability of some components is estimated from field data by a statistics-based approach, their limit-state functions are also unknown. Either case causes difficulties in accurately predicting the system reliability.

Several methods have been developed to address the above problem. The system reliability method in [7] deals with unknown details of outsourced components, and it assumes that the reliability function of an outsourced component with respect to various levels of component load is provided by the component supplier. The feasibility of integrating both physical- and statistics-approaches is investigated with some unknown limit-state functions for systems whose load is shared by its components and whose failure is due to excessive loading. In this area, two studies have been conducted for situations where some component parameters are recorded upon failure [5], or only the load parameters upon failure are collected [25]. The two- and one-class Support

Vector Machine methods [7, 25] are used for the two cases. Similar work has been performed for the re-evaluation of component reliability for a component when it is used in a new system with a different load [26]. These methods assume that the system load is shared by the components of the system and that the component loads have a linear relationship with the system load [27].

The objective of this work is to develop a new system reliability method for a system whose load is shared by its components. Different from the existing method, the component load can be a nonlinear function of the system load. For the components without limit-state functions, the component load is recorded once the component fails. The proposed method is more general than the existing methods because it does not assume a linear relationship between the component and system loads, and it requires less data.

The rest of this paper is organized as follows. Sec. 2 reviews FORM, and Sec. 3 discusses the proposed method, followed by examples in Sec. 4. Sec. 5 provides conclusions and suggests future work.

2. REVIEW OF FIRST-ORDER RELIABILITY METHOD (FORM)

FORM is a physics-based reliability method, which relies on a limit-state function defined by

$$Y = g(\mathbf{X}) \tag{2}$$

where Y is a response or state variable. If $Y < 0$, a failure occurs; otherwise, the component is safe. $\mathbf{X}$ is a vector of input random variables. The component reliability is calculated by

$$R = \Pr\{g(\mathbf{X}) \geq 0\} \tag{3}$$

Let the joint probability density function (PDF) of $\mathbf{X}$ be $f_{\mathbf{X}}(\boldsymbol{x})$. The associated probability of failure is obtained by integrating the PDF in the failure region $g(\boldsymbol{X}) < 0$ and is given by

$$p_f = 1 - R = \Pr\{g(\mathbf{X}) < 0\} = \int_{g(\boldsymbol{x})<0} f_{\mathbf{X}}(\boldsymbol{x})\, d\boldsymbol{x} \tag{4}$$

FORM approximates the integral in Eq. (4) by linearizing the failure boundary $g(\boldsymbol{X}) = 0$ using the first-order Taylor expansion. FORM involves the following three steps.

Step 1: Transform random variables into independent standard normal variables

$\mathbf{X} = (X_1, X_2, \dots, X_m)$ in the X-space is transformed into independent standard normal variables $\mathbf{U} = (U_1, U_2, \dots, U_m)$ in the U-space. If the components of $\mathbf{X}$ are independent, the transformation is given by [28]

$$F_i(X_i) = \Phi(U_i) \tag{5}$$

where $F_i(\cdot)$ and $\Phi(\cdot)$ are the cumulative distribution function (CDF) of X_i and U_i, respectively.

The transformation gives

$$X_i = F_i^{-1}\big(\Phi(U_i)\big) \tag{6}$$

We denote the transformation by $T(\cdot)$.

Step 2: Search for the most probable point (MPP)

The limit-state function is now

$$Y = g(\mathbf{X}) = g(T(\mathbf{U})) = G(\mathbf{U}) \tag{7}$$

At the limit state hypersurface $G(\boldsymbol{U}) = 0$, the point with the highest PDF value is called the MPP, denoted by $\mathbf{u}^*$. The MPP is obtained by

$$\mathbf{u}^* = \arg\min_{\mathbf{u}} \sqrt{\mathbf{u}\mathbf{u}^T}\,, \text{subject to } G(\mathbf{u}) = 0 \tag{8}$$

Then the limit-state function is linearized at the MPP, whose magnitude $\beta = \sqrt{\mathbf{u}^*(\mathbf{u}^*)^{\mathrm{T}}}$ is called the reliability index. The probability of failure is computed by

$$p_f = \Phi(-\beta) \tag{9}$$

3. METHODOLOGY

3.1 Overview

The proposed method is based on FORM. As discussed previously, this study deals with series systems, and the results can be easily extended to parallel systems. In this study, a component refers to a failure mode. A physical component may also be considered as a system because it may have multiple failure modes. For the purpose of system reliability analysis, a system may be a physical system or a physical component. For a series system, the system fails if any of its component fails or any of its failure mode occurs.

In this study, we assume that components fail due to excessive loading. The system load L is shared by components, and the load acting on the i-th component is denoted by L_i.

There are two types of components in the systems.

1) Components with predictable responses

The state of the component can be predicted by a limit-state function, which is defined by

$$Y_i^P = g_i(\mathbf{X}_i, L_i) \tag{10}$$

where Y_i^P is the response of component $i, i = 1,2, \dots, n_P$, in which n_P is the number of predictable components. $\mathbf{X}_i$ is a vector of random variables (except L_i) for the component, such as material properties and dimensions of the component. If $Y_i^P < 0$, a failure occurs. The probability of failure can be predicted by a physics-based reliability method such as FORM. The relationship between L and L_i is determined by a function $H_i(\cdot)$; namely

$$L_i = H_i(L) \tag{11}$$

$H_i(\cdot)$ may be a nonlinear function.

2) Components with observable responses

The state of the component Y_i^O, $i = 1,2,\dots,n_O$, with n_O being the number of observable responses, is observed in field or experiments, and the probability of failure is estimated from data collected. Common reliability engineering methodologies can be used to estimate the probability of failure. No limit-state function is available due to the lack of understanding of the physics of failure or outsourcing.

This study considers the most general problem where both types of components coexist in a system. The system designer has the following information.

- The component reliability R_i, $i = 1,2,\dots,n$. R_i is predicted by its limit-state function with a predictable response or is estimated by data with an observable response.
- Distribution of the system load L with PDF $f_L(l)$ and CDF $F_L(l)$.
- The failure data of the component load of an observable component. For a component with an observable response, the component load is collected or recorded when once the component fails.
- Limit-state functions and their input variables for components with predictable responses.

Instead of using the independence assumption in Eq. (1), the proposed method helps the system designer recover the missing dependence between all the component responses and their joint PDF, resulting in a more accurate system reliability prediction.

The key to the proposed method is to reconstruct equivalent limit-state functions for observable responses. We use FORM so that an equivalent limit-state function in the U-space is linear with respect to the component load and another random variable, which is a linear combination of all random input variables except the component load. Then all the responses can be modeled by a

multivariate normal distribution. The correlations of all the responses can then be found since only the component loads contribute to the correlations.

3.2 Reliability prediction for components with observable responses

Suppose the true limit-state function of an observable response is

$$Y_i^O = g_i(\mathbf{X}_i, L_i) = g_i(\mathbf{X}_i, H_i(L)) \tag{12}$$

where $\mathbf{X}_i$ is a vector of all the input random variables, except the component load, and the relationship between L and L_i is determined by a function $H_i(\cdot)$ in Eq. (11). The limit-state function is not available to the system designer. Data of the component load are collected from experiments or field. The recorded component load data are in a dataset $\boldsymbol{l}_i = (l_{i1}, l_{i2}, \dots, l_{id_i})$, where d_i is the size of the dataset. The probability of failure p_{fi} is estimated from the data.

At the limit state $Y_i^O = g_i(\mathbf{X}_i, L_i) = 0$, we solve for the component load L, and we have $L_i = g_i^{-1}(\mathbf{X}_i, Y_i^O)$, where $g_i^{-1}(\cdot)$ is the inverse function of $g_i(\cdot)$. The failure condition becomes $g_i^{-1}(\cdot) - L_i < 0$, where we consider $g_i^{-1}(\cdot)$ the general strength (capacity) of the component. As a result, we rebuild the equivalent limit-state function as

$$Y_i^O = C_i - L_i \tag{13}$$

where C_i is the general strength of the component $g_i^{-1}(\cdot)$ and is a function of $\mathbf{X}_i$.

C_i and L_i are independent. If $Y_i^O < 0$, or $C_i < L_i$, a failure occurs. Eq. (13) is based on the well-known stress and strength interference theory [29, 30], which applies to the systems whose failure is due to excessive loading.

With FORM, the limit-state function in the U-space becomes

$$\hat{Y}_i^O = \alpha_{C_i} U_{C_i} + \alpha_{L_i} U_{L_i} + \beta_i \tag{14}$$

where the reliability index β_i is derived from Eq. (9) as follows:

$$\beta_i = \Phi^{-1}(-p_{fi}) \tag{15}$$

When $\hat{Y}_i^O = \alpha_{C_i} U_{C_i} + \alpha_{L_i} U_{L_i} + \beta_i < 0$, a failure occurs. The reconstructed limit-state function is illustrated in Fig. 1.

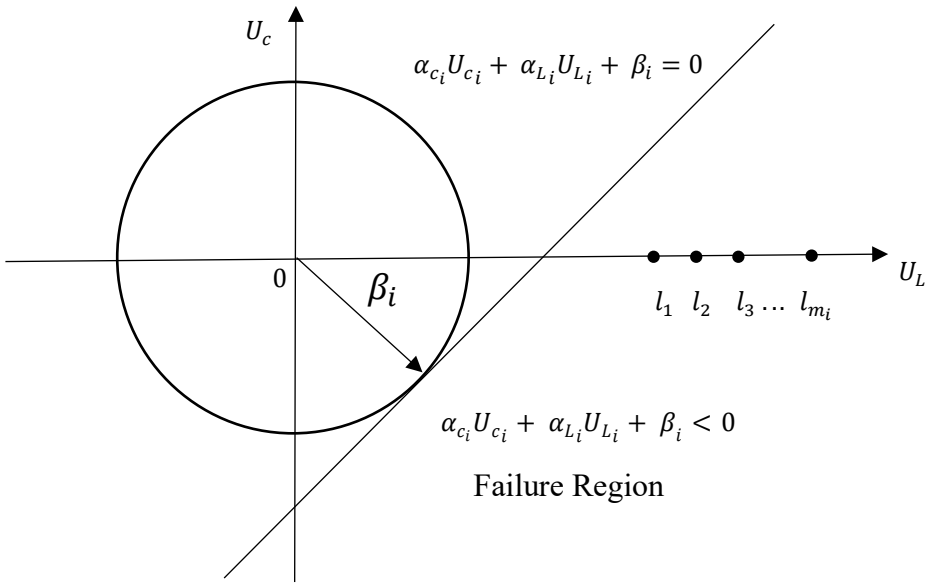

Fig. 1 Reconstructed limit-state function

The failure region is determined by $\alpha_{C_i} U_{C_i} + \alpha_{L_i} U_{L_i} + \beta_i < 0$. Let the random variables of the load U_L and capacity U_C in the failure region be U'_{L_i} and U'_{C_i}, respectively. They are conditional random variables given $\alpha_{C_i} U_{C_i} + \alpha_{L_i} U_{L_i} + \beta_i < 0$, or $U_{C_i} < -\frac{1}{\alpha_{C_i}}\left(\alpha_{L_i} U_{L_i} + \beta_i\right)$.

The joint PDF of U_{C_i} and U_{L_i} is $\phi(c)$, where $\phi(\cdot)$ is the PDF of a standard normal variable. The joint distribution of U'_C and U'_L is truncated by the safe region, and their joint PDF (defined in the failure region) is given by

$$f_{U'_{L_i}, U'_{C_i}}(l, c) = \begin{cases} \dfrac{\phi(c)\phi(l)}{p_{f_i}} & \text{if } \alpha_{C_i} U_{C_i} + \alpha_{L_i} U_{L_i} + \beta_i < 0 \\ 0 & \text{otherwise} \end{cases} \tag{16}$$

The joint PDF is plotted in Fig. 2.

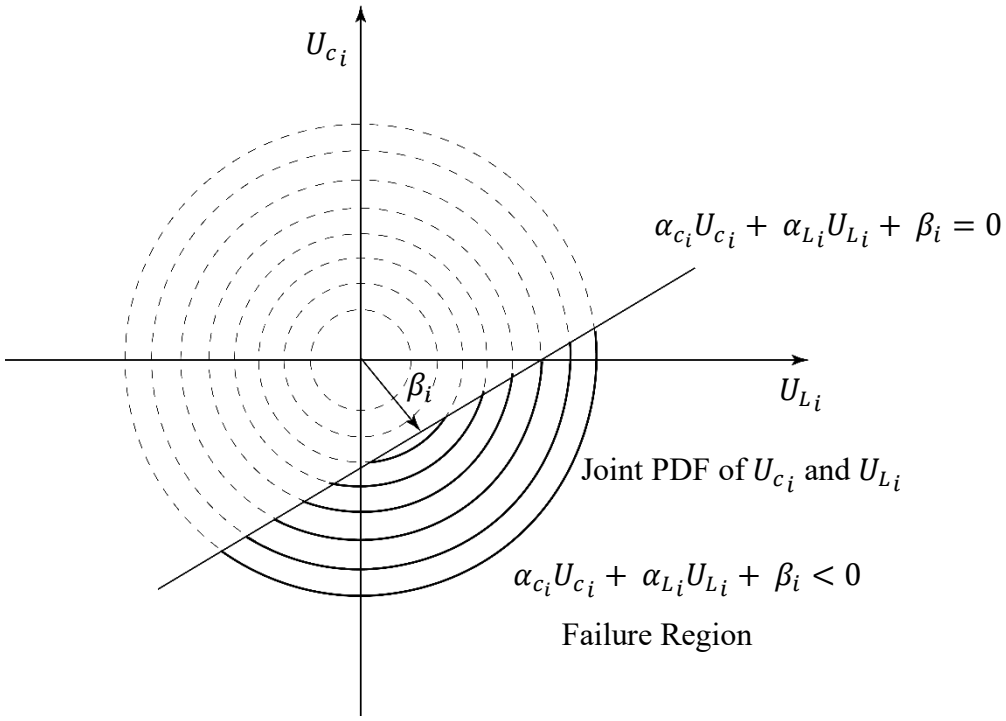

Fig. 2 Reconstructed equivalent limit-state function

Then the PDF of U_L' is given by

$$f_{U_{L_i}'}(l) = \int_{-\infty}^{+\infty} f_{U_L', U_C'}(l, c)dc = \int_{-\infty}^{-\frac{1}{\alpha_{C_i}}\left(\alpha_{L_i}U_{L_i}+\beta_i\right)} \frac{\phi(c)\phi(l)}{p_{fi}} dc$$
$$= \frac{1}{p_{fi}}\phi(l)\Phi\left(-\frac{\alpha_{L_i}l + \beta_i}{\alpha_{C_i}}\right) \quad (17)$$

Using $\alpha_{L_i}^2 + \alpha_{C_i}^2 = 1$, we have

$$f_{U_{L_i}'}(l) = \frac{1}{p_{fi}}\phi(l)\Phi\left(-\frac{\alpha_{L_i}l + \beta}{\sqrt{1-\alpha_{L_i}^2}}\right) \quad (18)$$

where $f_{U_{L_i}'}(l)$ is the conditional PDF of the component load in the failure region, and α_{L_i} is unknown. From the perspective of the Bayesian Theorem [31, 32], $f_{U_{L_i}'}(l)$ is the posterior PDF of

the component load given that a failure has occurred, and its unknown parameter α_{L_i} can be estimated from the observations or the samples of the component load. Transforming the load data $\boldsymbol{l}_i = (l_{1i,}, l_{i2}, \dots, l_{id_i})$ into the U-space, we obtain the sample of U'_{L_i}, $\boldsymbol{u}_{L_i} = (u_{L_i1}, u_{L_{i_2}}, \dots, u_{id_i})$. The likelihood function is defined by

$$V_{L_i} = \prod_{j=1}^{d_i} \phi(u_{L_ij}) \Phi\left(-\frac{\alpha_L u_{L_ij} + \beta_i}{\sqrt{1-\alpha_{L_i}^2}} \right) \tag{19}$$

Maximizing the likelihood function, we obtain α_{L_i}.

$$\alpha_{L_i} = \underset{-1 \le \alpha_{L_i} \le 0}{\arg\min} \prod_{j=1}^{d_i} \phi(u_{L_ij}) \Phi\left(-\frac{\alpha_L u_{L_ij} + \beta_i}{\sqrt{1-\alpha_{L_i}^2}} \right) \tag{20}$$

For computational convenience, we use the natural logarithm of the likelihood function, known as the log-likelihood function, as follows:

$$\alpha_{L_i} = \underset{-1 \le \alpha_{L_i} \le 0}{\arg\min} \sum_{j=1}^{d_i} \left\{ \phi \log(u_{L_ij}) + \log\left[\Phi\left(-\frac{\alpha_L u_{L_ij} + \beta_i}{\sqrt{1-\alpha_{L_i}^2}} \right) \right] \right\} \tag{21}$$

Eq. (21) presents a one-dimensional nonlinear optimization problem, and an analytical solution does not exist. A nonlinear programming algorithm can be used to solve it. In this work, we use the sequential quadratic programming method. To make sure a true optimal solution is found, we may use different starting points for α_{L_i}. If different answers are obtained, we should use the one that has the minimum objective function or $\sum_{j=1}^{d_i} \left\{ \phi \log(u_{L_ij}) + \log\left[\Phi\left(-\frac{\alpha_L u_{L_ij} + \beta_i}{\sqrt{1-\alpha_{L_i}^2}} \right) \right] \right\}$.

After α_{L_i} is found, the equivalent limit-state function in Eq. (14) is fully defined. Then the dependence between any two observable responses can be recovered. For example, for observable components *i* and *j*, the equivalent limit-state functions are

$$\begin{cases} \hat{Y}_i^O = \alpha_{S_i} U_{C_i} + \alpha_{L_i} U_{L_i} + \beta_i \\ \hat{Y}_j^O = \alpha_{S_j} U_{C_j} + \alpha_{L_j} U_{L_j} + \beta_j \end{cases} \tag{22}$$

Their covariance is

$$COV(\hat{Y}_i^O, \hat{Y}_j^O) = \alpha_{L_i} \alpha_{L_j} COV(U_{L_i}, U_{L_j}) \tag{23}$$

where $COV(\cdot)$ stands for covariance.

Recall that $L_i = H_i(L)$ and $L_j = H_j(L)$.

$$\begin{cases} U_{L_i} = \Phi^{-1}\left(F_L(L_i)\right) = \Phi^{-1}\left(F_L\left(H_i(L)\right)\right) \\ U_{L_j} = \Phi^{-1}\left(F_L\left(L_j\right)\right) = \Phi^{-1}\left(F_L\left(H_j(L)\right)\right) \end{cases} \tag{24}$$

Let U_L be the transformation of L in the U-space.

$$U_L = \Phi^{-1}\left(F_L(L)\right) \tag{25}$$

Assume that the component load L_i increases as system load L increases. Then $H_i(\cdot)$ is an increasing function. The CDF of L_i is given by

$$\begin{aligned} F_{L_i}(l_i) = \Pr\{L_i < l_i\} = \Pr\{H_i(L) < l_i\} = \Pr\{L < H_i^{-1}(l_i)\} \\ = F_L(H_i^{-1}(l_i)) = F_L(l) \end{aligned} \tag{26}$$

where $H_i^{-1}(\cdot)$ is the inverse of $H_i(\cdot)$, and $l = H_i^{-1}(l_i)$. Transforming L_i into U_{L_i}, we obtain

$$U_{L_i} = \Phi^{-1}\left(F_{L_i}(L_i)\right) = \Phi^{-1}\left(F_L(L)\right) \tag{27}$$

Using Eq. (24), we know that $U_{L_i} = U_L$. Similarly, we have $U_{L_j} = U_L$. As a result, $COV\left(U_{L_i}, U_{L_j}\right) = 1$, and

$$COV(\hat{Y}_i^O, \hat{Y}_j^O) = \alpha_{L_i}\alpha_{L_j} \tag{28}$$

Eq. (28) indicates how the relationship between component and system loads does not affect the covariance between two observable responses. This conclusion also holds for two predictable responses and a pair of observable and predictable responses. As a result, the proposed method can deal with any relationships between component and system loads if the function between the two types of loads is monotonically increasing.

3.3 Verifying covariance of two conservable responses

We now verify the conclusion in Sec. 3.2 with a linear case and a nonlinear case.

Case 1: Linear relationship between normally distributed component and system loads

Assume $L \sim N(\mu_L, \sigma_L^2)$, which means that L is normally distributed with a mean of μ_L and a standard deviation of σ_L. Also assume $L_i = k_i L$ and $L_j = k_j L$, where k_i and k_j are positive constants. Transforming L_i and L_j into U_{L_i} and U_{L_j}, we have

$$\begin{cases} U_{L_i} = \dfrac{k_i L - k_i \mu_L}{k_i \sigma_L} = \dfrac{L - \mu_L}{\sigma_L} \\ U_{L_j} = \dfrac{k_j L - k_j \mu_L}{k_j \sigma_L} = \dfrac{L - \mu_L}{\sigma_L} \end{cases} \tag{29}$$

This verifies $COV\left(U_{L_i}, U_{L_j}\right) = \frac{1}{\sigma_L^2} COV(L, L) = 1$.

Case 2: Nonlinear relationship between a component and the system load

The verification is given in Example 1 in Sec. 4.

3.4 System reliability prediction

After the equivalent limit-state functions of observable responses are constructed, the limit-state functions of all the components will be available to the system designer. With the use of FORM, all the limit-state functions in the U-space are given by

$$\begin{aligned} \hat{Y}_i^P &= \alpha_{C_i} U_{C_i} + \alpha_{L_i} U_{L_i} + \beta_i, i = 1,2,\dots,n_P \\ \hat{Y}_j^O &= \alpha_{C_j} U_{C_j} + \alpha_{L_j} U_{L_j} + \beta_j, i = 1,2,\dots,n_O \end{aligned} \tag{30}$$

Then all the responses are assembled into $\hat{\mathbf{Y}} = (\hat{\mathbf{Y}}^P, \hat{\mathbf{Y}}^O)$, where $\hat{\mathbf{Y}}^P = (\hat{Y}_1^P, \hat{Y}_2^P, \dots, \hat{Y}_{n_P}^P)$ and $\hat{\mathbf{Y}}^O = (\hat{Y}_1^O, \hat{Y}_2^O, \dots, \hat{Y}_{n_P}^O)$. It can be shown that $\hat{\mathbf{Y}}$ follows a n-dimensional multivariate normal distribution $\hat{\mathbf{Y}} \sim N_n(\boldsymbol{\mu}, \boldsymbol{\Sigma})$, where $n = n_P + n_O$, $\boldsymbol{\mu}$ is the mean vector, and $\boldsymbol{\Sigma}$ is the covariance matrix.

$$\boldsymbol{\mu} = (\boldsymbol{\mu}^P, \boldsymbol{\mu}^O) = \left(\beta_1^P, \beta_2^P, \dots, \beta_{n_P}^P, \beta_1^O, \beta_2^O, \dots, \beta_{n_O}^O\right) \tag{31}$$

where

$$\boldsymbol{\mu}^P = \left(\beta_1^P, \beta_2^P, \dots, \beta_{n_P}^P\right) \tag{32}$$

and

$$\boldsymbol{\mu}^O = \left(\beta_1^O, \beta_2^O, \dots, \beta_{n_O}^O\right) \tag{33}$$

The covariance matrix is

$$\boldsymbol{\Sigma} = \begin{pmatrix} \boldsymbol{\Sigma}^{PP} & \boldsymbol{\Sigma}^{PO} \\ \boldsymbol{\Sigma}^{OP} & \boldsymbol{\Sigma}^{OO} \end{pmatrix} \tag{34}$$

with sizes of $\begin{pmatrix} n_P \times n_P & n_P \times n_O \\ n_O \times n_P & n_O \times n_O \end{pmatrix}$.

$$\boldsymbol{\Sigma}^{PP} = \left(COV\left(\hat{Y}_i^P, \hat{Y}_j^P\right)\right)_{i,j=1,2,\dots,n_P} \tag{35}$$

$$\boldsymbol{\Sigma}^{OO} = \left(COV\left(\hat{Y}_i^O, \hat{Y}_j^O\right)\right)_{i,j=1,2,\ldots,n_O} \tag{36}$$

$$\boldsymbol{\Sigma}^{PO} = \left(COV\left(\hat{Y}_i^P, \hat{Y}_j^O\right)\right)_{i=1,2,\ldots,n_P, j=1,2,\ldots,n_O} \tag{37}$$

The elements of the covariance matrix are given by

$$COV(\hat{Y}_i^P, \hat{Y}_j^O) = \alpha_{L_i}\alpha_{L_j} \tag{38}$$

$$COV(\hat{Y}_i^P, \hat{Y}_j^O) = \alpha_{L_i}\alpha_{L_j} \tag{39}$$

$$COV(\hat{Y}_i^O, \hat{Y}_j^O) = \alpha_{L_i}\alpha_{L_j} \tag{40}$$

The system reliability is then calculated by

$$R_S = \Pr\left(\bigcap_{i=1}^{n} \hat{Y}_i > 0\right) = \Pr\left(\bigcap_{i=1}^{n} -Y_i < 0\right) \tag{41}$$

The joint PDF and CDF of $-\hat{\mathbf{Y}}$ be $\phi_n(\hat{\mathbf{y}}; -\boldsymbol{\mu}, \boldsymbol{\Sigma})$ and $\Phi_n(\hat{\mathbf{y}}; -\boldsymbol{\mu}, \boldsymbol{\Sigma})$, respectively; then

$$R_S = \Phi_n(\mathbf{0}; -\boldsymbol{\mu}, \boldsymbol{\Sigma}) = \int_{-\infty}^{0} \cdots \int_{-\infty}^{0} \phi_n(\boldsymbol{y}; -\boldsymbol{\mu}, \boldsymbol{\Sigma})\, d\boldsymbol{y} \tag{42}$$

Numerical methods [33-36] or MCS can be used to calculate the multivariate integral in Eq. (42).

The accuracy of the reliability prediction can be improved if a more accurate component reliability method such as MCS is used. This can be achieved with a more accurate component reliability prediction for predictable responses. If we have a more accurate result of the probability of failure p_{fj} of the *j*-th component with a predictable response, we can use p_{fj} to obtain reliability index β_j with higher accuracy in Eq. (30) using Eq. (15); namely, $\beta_j = \Phi^{-1}(-p_{fj})$.

4. EXAMPLES

In this section, four examples are used to demonstrate the proposed methods. Example 1 verifies that the covariance between two component loads in the U-space is equal to 1 as discussed in Sec. 3.2. Example 2 provides a step-by-step demonstration to show how the unknown covariance between two observable responses is recovered by the Bayesian approach. Example 3 shows how to calculate the probability of system failure in a mechanical system with two types of components. Example 4 involves a mechanical system with more components and random variables.

4.1 Example1: Estimation and verification of covariance between two component loads

A system load L follows a lognormal distribution, denoted by $L \sim LN(u_L, {\sigma_L}^2)$, with a mean and a standard deviation of $u_L = 6.9027$ and $\sigma_L = 0.09975$, respectively. The component loads of two components are given by

$$\begin{cases} L_1 = H_1(L) = L^{2/3} + 1 \\ L_2 = H_2(L) = 3L^{0.5} - 1 \end{cases} \tag{43}$$

We now use MCS to demonstrate that the covariance between component loads U_{L_1} and U_{L_2} is 1 even though the functions in Eq. (43) are nonlinear.

We first generate samples of L with a sample size of 10^5. By plugging the samples of L into Eq. (43), we get the samples of L_1 and L_2. The empirical CDF of L_1 and L_2, denoted by $F_{L_1}(l_1)$ and $F_{L_2}(l_2)$, respectively, are estimated and are shown in Figs. 3 and 4. Then transforming the load data L_1 and L_2 into the U-space by $U_{L_i} = \Phi^{-1}\left(F_{L_i}(l_i)\right), i = 1, 2$, we obtain samples U_{L_1} and U_{L_2}. We then use the samples to estimate the covariance of U_{L_1} and U_{L_2}. The flowchart is given in Fig. 5.

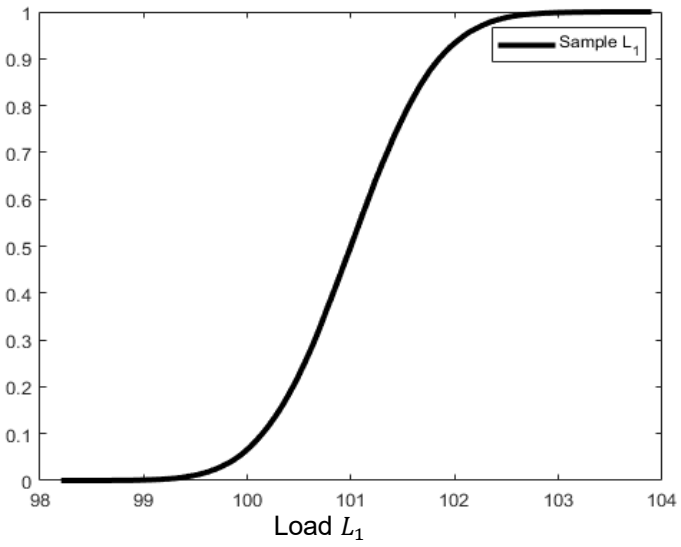

Fig. 3 Empirical CDF of L_1

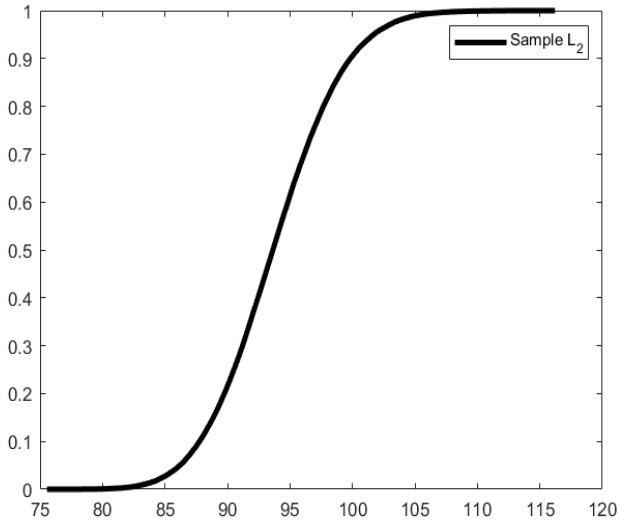

Fig. 4 Empirical CDF of L_2

The covariance of U_{L_1} and U_{L_2} is found to be $COV(U_{L_1}, U_{L_2}) = 1.0077$, which is close to the true value of 1. Note that the covariance cannot exceed 1. $COV(U_{L_1}, U_{L_2})$ is slightly greater than 1 due to an accumulative numerical error.

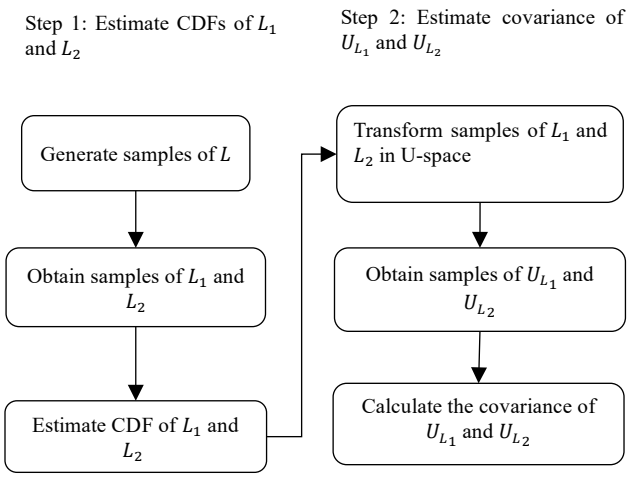

Fig. 5 Flow chart of estimating the covariance

4.2 Example 2: A mathematical problem

The limit-state function of a component with an observable response in the U-space is given by

$$\hat{Y} = \alpha_1 U_1 + \alpha_2 U_2 + \alpha_3 U_3 + \alpha_L U_L + \beta \tag{44}$$

where U_L is the component load, and U_i $(i = 1, 2, 3)$ are other random variables, and $\beta = 3.5$. The unit vector is given by $\boldsymbol{\alpha} = (\alpha_1, \alpha_2, \alpha_3, \alpha_L) = (0.8165, 0.1361, -0.1361, -0.5443)$, and the last component is for the component load; namely, $\alpha_L = -0.5443$.

Now we use the proposed method to estimate α_L and compare it with the true value -0.5443. To mimic the physical experiment, we conduct the experiment on computer. In other words, we use MCS and the true limit-state function to generate samples of the component load L in the failure region. The details are as follows. We generate 30 random samples of all the random variables U_1, U_2, U_3, and U_L; at these sample points, we have response $\hat{Y} < 0$. This mimics the component failure. Then the 30 samples of U_L represent the data of component load recorded when the component failed. We then use the maximum likelihood method in Eq. (19) to estimate α_L.

Since the above process involves random sampling and the result contains variation, we repeat the same process 30 times. The estimated α_L from the 30 runs are given in Table 1.

The mean and standard deviation of α_L are $\mu_{\alpha_L} = -0.5372$ and $\sigma_{\alpha_L} = 0.0580$, respectively. Comparing $\mu_{\alpha_L} = -0.5372$ with the true value -0.5443, we see that they are in good agreement.

Table 1 Estimates of α_L

-0.6199	-0.6293	-0.5561	-0.5468	-0.5769
-0.5160	-0.6190	-0.5438	-0.6216	-0.5575
-0.5655	-0.5569	-0.5378	-0.5866	-0.5391
-0.5417	-0.6255	-0.6037	-0.4839	-0.4825
-0.5876	-0.5617	-0.4753	-0.6197	-0.5441
-0.5859	-0.4413	-0.5473	-0.5473	-0.5920

4.3 Example 3: A system with two shafts

A system consists of two shafts as shown in Fig. 6. Both shafts share the system load $L = F$. L follows a normal distribution $N(3000, 660^2)$ N. The component loads of the shafts 1 and 2 are given by $L_1 = 0.7L$ and $L_2 = 0.3L$, respectively.

Shaft 1 has a predictable response, and its limit-state function is available and is given by

$$Y_1 = g_1(\mathbf{X}_1, L_1) = S_1 - \frac{16}{\pi d_1^3}\sqrt{4L_1^2 l^2 + 3T_1^2} \tag{45}$$

where S_1 is the yield strength of the shaft, T_1 is the torque applied to the shaft, $d_1 = 39$ mm is the diameter of the shaft, and $l = 600$ mm is the length of the shaft. $\mathbf{X}_1 = (S_1, T_1)$.

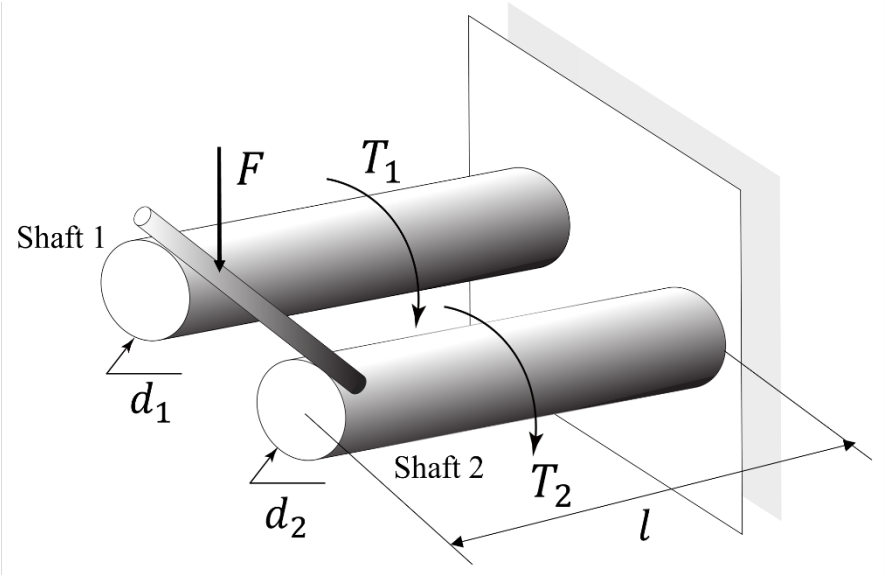

Fig. 6 A system with two shafts

The distributions of S_1 and T_1 are $N(250, 6^2)$ MPa and $N(450,20^2)$ N·m, respectively. The system designer uses FORM to perform the reliability analysis, which yields the reliability index $\beta_1 = 2.9873$ and the limit-state function in the U-space $Y_1^P = \alpha_{11}U_{S_1} + \alpha_{12}U_{T_1} + \alpha_{L_1}U_{L_1} - \beta_1$, where $\boldsymbol{\alpha}_1 = [\alpha_{11}, \alpha_{12}, \alpha_{L_1}] = [0.192752, -0.02602, -0.9809]$.

The limit-state function of shaft 2 is unknown, and the shaft has an observable response. Its reliability is estimated by data. Assume the true limit-state function is given by

$$\hat{Y}_2^{true} = g_2(\mathbf{X}_2, L_2) = S_2 - \frac{16}{\pi d_2^3}\sqrt{4L_2^2 l^2 + 3T_2^2} \tag{46}$$

where S_2 is the yield strength of the shaft, T_2 is the torque applied to the shaft, $d_1 = 39$ mm is the diameter of the shaft, and $l = 600$ mm is the length of the shaft. $\mathbf{X}_2 = (S_2, T_2)$. The distributions of S_2 and T_2 are $N(130, 8^2)$ MPa and $N(450,20^2)$ N·m, respectively. The reliability of shaft 2 is estimated by experimental data. We use MCS to mimic the experiment by using the true limit-state function in Eq. (46). The reliability index obtained is $\beta_2 = 2.9642$. The system designer then

reconstructs an equivalent limit-state function $Y_2^O = \alpha_{S_2} U_{S_2} + \alpha_{L_2} U_{L_2} - \beta_2$. The system designer uses the proposed Bayesian approach with 17 samples of L_2 in the failure region (in the U-space) to estimate the unknown coefficient α_{L_2}, and the result is $\alpha_{L_2} = -0.8062$. The true coefficient from the true limit-sate function in Eq. (46) is $\alpha_{L_2}^{true} = -0.8028$.

The system designer now has the following information: The mean vector $\boldsymbol{\mu} = (\mu_1, \mu_2) = (-2.1313, -3.1224)$, and the covariance $cov(\hat{Y}_1^P, \hat{Y}_2^O) = \alpha_{L_1}\alpha_{L_2} = 0.80$, which results in the covariance matrix $\boldsymbol{\Sigma} = \begin{pmatrix} 1 & 0.80 \\ 0.80 & 1 \end{pmatrix}$. This indicates a strong correlation between the two responses. The system probability of failure estimated by the system designer using Eq. (42) is $p_{fs} = 1 - R = 1 - \Phi_2(\mathbf{0}; -\boldsymbol{\mu}, \boldsymbol{\Sigma}) = 2.534 \times 10^{-3}$. The result from the independent component assumption and the true value are given in Table 2. The true probability of failure is estimated from MCS using all the limit-state functions with a sample size of 10^6. The results show that the proposed method is more accurate than the traditional method.

Table 2 The probabilities of system failure

Method	p_{fs}	ε %
Proposed method	2.5348×10^{-3}	0.9
Independence assumption method	2.9227×10^{-3}	14.2
MCS	2.5580×10^{-3}	N/A

In this example, Y_1 is a predictable response, whose reliability is calculated numerically with FORM. The number of limit-state function calls is usually used as a measure of computational efficiency. The number of function calls for Y_1 is 16.

We now use this example to discuss possible errors in the system reliability prediction. The errors are from 1) the use of FORM, 2) the limited failure data for observable responses, and 3) the ignorance of the dependence between components.

To show the first error due to the use of FORM, we compare the result from FORM using the true correlation coefficient with the accurate solution. The solution is 2.5347×10^{-3}, and the error is 0.9% compared to the accurate 2.5580×10^{-3}. The error from FORM in this problem is therefore small.

To examine the second error due to the random data, we ran the problem 30 times with different random failure data with the same sample size 17. The average solution is 2.5282×10^{-3} with an average error 1.2%. The standard deviation is 8.3677×10^{-5}, which is small, indicating the relatively small error due to the randomness of the failure data.

For the third error due to the ignorance of the dependence between components, we have already provided the results in Table 2. The table indicates that the error from the independence assumption method is large.

4.4 Example 4: A connector assembly

A connector assembly system consists of a rectangular steel bar, and a steel channel is assembled by four identical bolts at points A, B, C and D as shown in Fig. 7 [37]. The external load F, which is the system load L, acts at the end of the bar.

There are six physical components in the system, where the steel bar and the channel are in-house designed and manufactured, and the four bolts are purchased from a component supplier. The reliability of the in-house components is predicted by a physics-based approach, and the reliability of the outsourced bolts is estimated by data. Hence the responses of the three former components are predictable, and the responses of the latter four components are observable.

The distributions of random variables known to the system designer are given in Table 3, and they include the distributions of F and those associated with the in-house components. The limit-state functions of the two in-house components are derived below.

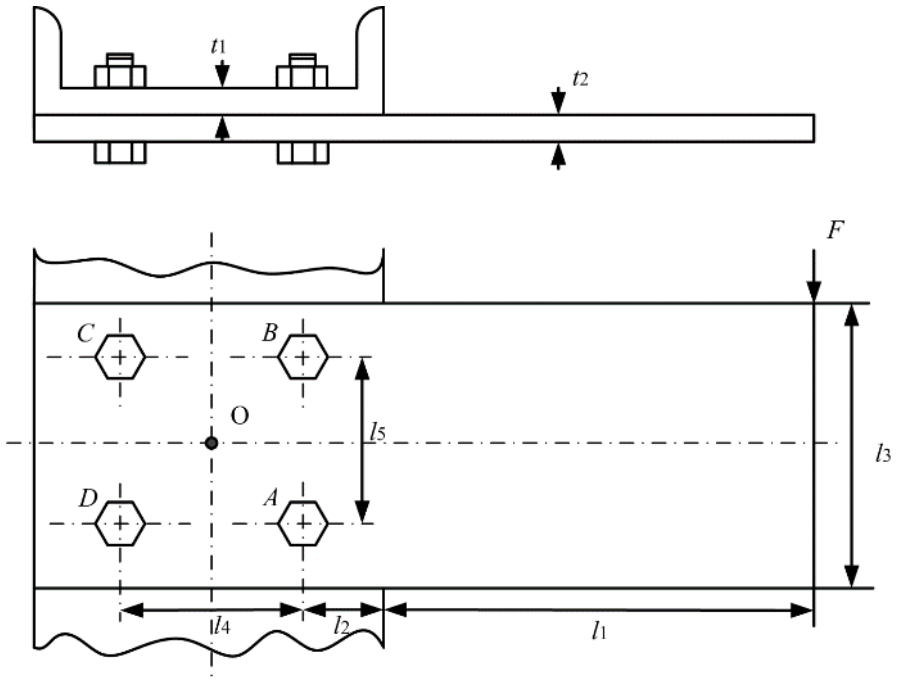

Fig. 7 A connector assembly

Table 3 Distributions associated with predictive responses

Variable	Description	Distribution
F (N)	External force	$N(1.8 \times 10^4, 3.36 \times 10^3)$
d_1 (m)	Channel hole *D* inner diameter	$N(1.6 \times 10^{-3}, 3.2 \times 10^{-4})$
d_2 (m)	Bar hole *D* inner diameter	$N(1.6 \times 10^{-3}, 3.2 \times 10^{-4})$
S (Pa)	Channel yield strength	$N(300 \times 10^6, 24 \times 10^6)$
S_2 (Pa)	Bar yield strength	$N(300 \times 10^6, 24 \times 10^6)$
t_1 (Pa)	Channel thickness	$N(1.0 \times 10^{-3}, 2.0 \times 10^{-5})$
t_2 (Pa)	Bar thickness	$N(1.0 \times 10^{-3}, 2.0 \times 10^{-5})$
l_1 (m)	See Fig. 7	$N(3.2 \times 10^{-1}, 6.4 \times 10^{-3})$
l_2 (m)	See Fig. 7	$N(5.0 \times 10^{-1}, 1.0 \times 10^{-3})$
l_3 (m)	Bar width	$N(2.0 \times 10^{-1}, 4.0 \times 10^{-3})$
l_4 (m)	Distance between bolts *A* and *D*; and *B* and *C*	$N(7.5 \times 10^{-2}, 1.5 \times 10^{-3})$
l_5 (m)	Distance between bolts *A* and *B*; and *C* and *D*	$N(6.0 \times 10^{-4}, 1.2 \times 10^{-3})$

Since the four bolts are symmetrically installed and are equally distanced from the centroid point O, the distance from each bolt to the centroid is $r = 0.5\sqrt{l_4^2 + l_5^2}$. The shear reaction V and

moment reaction M at O are given by $V = F$ and $M = F\left(l_1 + l_2 + \frac{l_4}{2}\right)$, respectively. The primary shear load per bolt is $F' = \frac{V}{4}$, and the secondary shear forces are equal and are given by $F'' = \frac{Mr}{4r^2} = \frac{M}{4r}$. By applying the parallelogram rule, we obtain the magnitudes of the primary and the secondary shear forces as follows.

$$F_A = F_B = \sqrt{(F')^2 + (F'')^2 - 2F'F''cos\theta_1} \tag{47}$$

$$F_C = F_D = \sqrt{(F')^2 + (F'')^2 - 2F'F''cos\theta_2} \tag{48}$$

where $\theta_1 = \frac{pi}{2} + \arctan\left(\frac{l_4}{l_5}\right)$, and $\theta_2 = \frac{pi}{2} - \arctan\left(\frac{l_4}{l_5}\right)$.

The channel has one failure mode caused by excessive bearing stress. The bearing area of the channel is $A_1 = t_1 d_1$, where d_1 is the inner diameter of the hole D in the channel. $L_1 = F_A$ and $\mathbf{X}_1 = (S_1)$. The limit-state function is given by

$$Y_1 = g_1(\mathbf{X}_1, L_1) = \frac{F_A}{A_1} - S_1 \tag{49}$$

The bar is another in-house component. It has two failure modes. The first one is due to an excessive bearing stress, and the associated limit-state function is given by

$$Y_2 = g_2(\mathbf{X_2}, L_2) = \frac{F_A}{A_2} - S_2 \tag{50}$$

in which $A_2 = t_2 d_2$, where d_2 is the inner diameter of hole B of the bar, S_2 is the yield strength. $L_2 = F_A$, and $\mathbf{X}_2 = (S_2)$. The second failure mode occurs due to the excessive bending stress at the cross section A-B, whose moment of inertia of the cross section is given by

$$I = I_{bar} - 2\left(I_{holes} + \bar{d}^2 A\right) = \frac{t_2 l_2^3}{12} - 2\left[\frac{t_2 d_a^3}{12} + \frac{l_5^3}{4} t_2 d_a\right] \tag{51}$$

and the limit-state function is defined by

$$Y_3 = g_3(\mathbf{X_3}, L_3) = \frac{M_1}{I/c} - S_2 \tag{52}$$

in which I/c is the section modulus, $c = l_3/2$, and $M_1 = F(l_1 + l_2)$ is the bending moment.

We now discuss the outsourced components. Bolts A, B, C and D are components with observable responses, and the system designer does not know their failure modes and limit-state functions. Experiments on the individual bolts are performed until the bolts fail, and the values of the force F are recorded upon failure. Their reliability is estimated from the experimental results. To mimic the actual physical experiments and simulate the experiments. we use their true limit-state functions, which are given by

$$\hat{Y}_4^{true} = g_4^{true}(\mathbf{X_4}, L_4) = \frac{F_A}{A_{sa}} - \tau_a \tag{53}$$

$$\hat{Y}_5^{true} = g_5^{true}(\mathbf{X_5}, L_5) = \frac{F_B}{A_{sb}} - \tau_b \tag{54}$$

where A_{sa} and A_{sb} are the areas subject to shear stresses, and τ_a and τ_b are the allowable shear stresses of bolt A and B, respectively. $\mathbf{X_4} = (A_{sa}, \tau_a)$, $L_4 = F_A$. $\mathbf{X_5} = (A_{sb}, \tau_b)$, $L_5 = F_B$.

$$\hat{Y}_6^{true} = g_6^{true}(\mathbf{X_6}, L_6) = \frac{F_C}{A_{sc}} - \tau_c \tag{55}$$

$$\hat{Y}_7^{true} = g_7^{true}(\mathbf{X_7}, L_7) = \frac{F_D}{A_{sd}} - \tau_d \tag{56}$$

where A_{sc} and A_{sd} are areas subject to shear stresses, and τ_c and τ_d are the allowable shear stresses of bolts C and D, respectively. $\mathbf{X}_6 = (A_{sc}, \tau_c)$, $L_6 = F_C$. $\mathbf{X}_7 = (A_{sd}, \tau_d)$, $L_7 = F_D$. We also use the true distributions associated with the outsourced variables to simulate the experiments. The distributions are given in Table 4.

With the above true limit-state functions, we use MCS to generate samples of all the random variables in Table 4 and estimate the reliability of the four components. The reliability of each of the bolts is assumed from experiments. We also pick 17 random samples of the force F in the failure region and assume that they are the recorded samples from the experiments.

Table 4 Distributions associated with observable responses

A_{sa} (m^2)	Bolt A shear-stress area	$N(1.44 \times 10^{-4}, 2.88 \times 10^{-6})$
A_{sb} (m^2)	Bolt B shear-stress area	$N(1.44 \times 10^{-4}, 2.88 \times 10^{-6})$
A_{sc} (m^2)	Bolt C shear-stress area	$N(1.15 \times 10^{-4}, 2.88 \times 10^{-6})$
A_{sd} (m^2)	Bolt D shear-stress area	$N(1.15 \times 10^{-4}, 2.88 \times 10^{-6})$
τ_a (Pa)	Bolt A allowable shear stress	$LN(310 \times 10^6, 24.8 \times 10^6)$
τ_b (Pa)	Bolt B allowable shear stress	$LN(310 \times 10^6, 24.8 \times 10^6)$
τ_c (Pa)	Bolt C allowable shear stress	$LN(310 \times 10^6, 24.8 \times 10^6)$
τ_d (Pa)	Bolt D allowable shear stress	$LN(310 \times 10^6, 24.8 \times 10^6)$
d_a (m)	Bolt A diameter	$N(1.6 \times 10^{-2}, 6.4 \times 10^{-4})$
d_b (m)	Bolt B diameter	$N(1.6 \times 10^{-2}, 6.4 \times 10^{-4})$
d_c (m)	Bolt C diameter	$N(1.6 \times 10^{-2}, 3.2 \times 10^{-4})$
d_d (m)	Bolt D diameter	$N(1.6 \times 10^{-2}, 3.2 \times 10^{-4})$

From the estimated reliability, the system designer calculates the reliability indexes and reconstructs the equivalent limit-state functions as follows.

$$\hat{Y}_i^O = \alpha_{S_i} U_{S_i} + \alpha_{L_i} U_{L_i} + \beta_i \ (i = 4, \dots, 7)$$

in which $\beta_4 = 3.4914$, $\beta_5 = 3.4914$, $\beta_6 = 4.1971$, $\beta_7 = 4.1971$.

Using β_i $(i = 4, \dots, 7)$ and the proposed Bayesian approach, the system designer estimates the unknown coefficients α_{L_i} and obtain $\alpha_{L_4} = -0.8316$, $\alpha_{L_5} = -0.8475$, $\alpha_{L_6} = -0.7675$, $\alpha_{L_7} = -0.8536$. Their true values from the assumed true limit-state function are $\alpha_{L_4}^{(true)} = -0.8229$,

$\alpha_{L_5}^{(true)} = -0.8229$, $\alpha_{L_6}^{(true)} = -0.7980$ and $\alpha_{L_7}^{(true)} = -0.7980$. The results show that the estimated coefficients are close to the true ones.

Using the estimated coefficients, the system designer obtains the covariance matrix as follows.

$$\boldsymbol{\Sigma} = \begin{bmatrix} 1.0 & 0.6134 & \cdots & 0.5966 & 0.6618 \\ 0.6134 & 1.0 & \cdots & 0.6263 & 0.6948 \\ \vdots & \vdots & \ddots & \vdots & \vdots \\ 0.5966 & 0.6263 & \cdots & 1.0 & 0.6789 \\ 0.6618 & 0.6948 & \cdots & 0.6789 & 1.0 \end{bmatrix}_{7\times 7}$$

The mean vector is

$$\boldsymbol{\mu} = (\beta_1, \beta_2, \dots, \beta_7) = (3.8461, 3.8461, 3.7545, 3.4914, 3.4914, 4.1971, 4.1971)$$

Plugging $\boldsymbol{\mu}$ and $\boldsymbol{\Sigma}$ into Eq. (42), the system designer predicts the probability of system failure, and the result is given in Table 5. The result from the independence assumption method is also provided in the table. MCS is used to produce a true prediction with the assumption that all the limit-state functions $g_i(\cdot)$ $(i = 1, 2, 3)$ and $g_j^{true}(\cdot)$ $(j = 4, 5, 6, 7)$ are known. The sample size of MCS is 10^6. The error of the proposed method is 4.3%, much smaller than the error from the independence assumption method, which is approximately 19.5%.

Table 5 The probabilities of system failure

Method	p_f	ε %
Proposed method	5.7179×10^{-4}	4.3
Independence assumption method	7.1418×10^{-4}	19.5
MCS	5.9760×10^{-4}	N/A

Table 6 The number of function evaluations

Limit-state function	Function calls
Y_1	100
Y_2	100
Y_3	125

In this example, Y_1, Y_2, and Y_3 are predictable responses. Their reliability is calculated numerically with FORM. The number of function calls for Y_1, Y_2, and Y_3 are 100, 100, and 125, respectively.

5. CONCLUSIONS

This study considers the reliability prediction for series systems with both predictable and observable component responses. The proposed method is applicable for systems whose load is shared by its components and whose failure is due to excessive loading. The results demonstrate that it is possible to reconstruct an equivalent limit-state function for an observable component response if the load that causes a failure is recorded upon failure with a set of samples. The unknown coefficient of the component load in the equivalent limit-state function can be obtained by the maximum likelihood estimate with the proposed Bayesian approach. The joint PDF of all the component responses is then obtainable with the availability of all the limit-state functions of predictable and observable components responses, thereby leading to a more accurate system reliability prediction than the traditional method that assumes independent component states. The other advantage of the proposed method is that it can deal with any relationships between system and component loads, including nonlinear relationships.

The method is limited to systems with only one system load. If multiple system loads exist, the equivalent limit-state function should include multiple component loads that correspond to the system loads, and there will be multiple unknown coefficients for the component loads. Our future work will focus on estimating the unknown coefficients by the proposed Bayesian approach. Once the coefficients are available, the joint distribution of all the components can then be obtained using the same approach developed in this study.

ACKNOWLEDGEMENTS

We would like to acknowledge the support from the National Science Foundation under Grants No. 1923799 and No. 1924413. Author Li would also like to thank the support from Indiana University–Purdue University Indianapolis.

REFERENCES

[1] Bae, S., Kim, N.H. and Jang, S.G., 2019, "System reliability-based design optimization under tradeoff between reduction of sampling uncertainty and design shift," Journal of Mechanical Design, 141(4), p.041403.

[2] Liang, J., Mourelatos, Z. P., and Nikolaidis, E., 2007, "A single-loop approach for system reliability-based design optimization," Journal of Mechanical Design, 129(12), pp. 1215-1224.

[3] Jung, Y., Kang, K., Cho, H., and Lee, I., 2021, "Confidence-based Design Optimization (CBDO) for a More Conservative Optimum under Surrogate Model Uncertainty Caused by Gaussian Process," Journal of Mechanical Design, 143(9), p.091701.

[4] Xi, Z., 2019, "Model-based reliability analysis with both model uncertainty and parameter uncertainty," Journal of Mechanical Design, 141(5), p.051404

[5] Hu, Z., and Du, X., 2018, "Integration of Statistics-and Physics-Based Methods—A Feasibility Study on Accurate System Reliability Prediction," Journal of Mechanical Design, 140(7), p. 074501.

[6] O'Connor, P., and Kleyner, A., 2012, Practical reliability engineering, John Wiley & Sons.

[7] Hu, Z., and Du, X., 2017, "System reliability prediction with shared load and unknown component design details," Artificial Intelligence for Engineering Design, Analysis and Manufacturing, 31(3), pp. 223-234.

[8] Chiralaksanakul, A., and Mahadevan, S., 2004, "First-Order Approximation Methods in Reliability-Based Design Optimization," Journal of Mechanical Design, 127(5), pp. 851-857.

[9] Du, X., and Hu, Z., 2012, "First order reliability method with truncated random variables," Journal of Mechanical Design, 134(9), p.091005.

[10] Chiralaksanakul, A., and Mahadevan, S., 2005, "First-order approximation methods in reliability-based design optimization," Journal of Mechanical Design, 127(5), pp. 851-857.

[11] Zhao, Y., and Ono, T., " A general procedure for first/second-order reliabilitymethod (FORM/SORM)," Structural safety, 21(2), pp.95-112.

[12] Lee, I., Noh, Y., and Yoo, D., 2012, "A novel second-order reliability method (SORM) using noncentral or generalized chi-squared distributions," Journal of Mechanical Design, 134(10), p.100912.

[13] Mansour, R., and Olsson, M., 2014, "A closed-form second-order reliability method using noncentral chi-squared distributions," Journal of Mechanical Design, 136(10), p.100912.

[14] Choi, S.-K., Grandhi, R., and Canfield, R. A., 2006, Reliability-based structural design, Springer Science & Business Media.

[15] Zhu, Z., and Du, X., 2016, "Reliability analysis with Monte Carlo simulation and dependent Kriging predictions," Journal of Mechanical Design, 138(12), p.121403.

[16] Du, X., and Sudjianto, A., 2004, "First order saddlepoint approximation for reliability analysis," AIAA journal, 42(6), pp. 1199-1207.

[17] Papadimitriou, D. I., and Mourelatos, Z. P., 2018, "Reliability-based topology optimization using mean-value second-order saddlepoint approximation," Journal of Mechanical Design, 140(3), p.031403.

[18] Papadimitriou, D. I., Mourelatos, Z. P., and Hu, Z., 2019, "Reliability analysis using second-order saddlepoint approximation and mixture distributions," Journal of Mechanical Design, 141(2), p.021401.

[19] Du, X., 2008, "Saddlepoint approximation for sequential optimization and reliability analysis," Journal of Mechanical Design, 130(1), p.011011.

[20] Jin, R., Du, X., and Chen, W., 2003, "The use of metamodeling techniques for optimization under uncertainty," Structural and Multidisciplinary Optimization, 25(2), pp. 99-116.

[21] Wang, Y., Hong, D., Ma, X., and Zhang, H., 2018, "A radial-based centralized kriging method for system reliability assessment," Journal of Mechanical Design, 140(7), p.071403.

[22] Wu, H., Zhu, Z., and Du, X., 2020, "System Reliability Analysis With Autocorrelated Kriging Predictions," Journal of Mechanical Design, 142(10), p.101702.

[23] Du, X., 2010, "System reliability analysis with saddlepoint approximation," Structural and Multidisciplinary Optimization, 42(2), pp. 193-208.

[24] Hohenbichler, M., and Rackwitz, R., 1982, "First-order concepts in system reliability," Structural safety, 1(3), pp. 177-188.

[25] Hu, Z., Hu, Z., and Du, X., 2019, "One-class support vector machines with a bias constraint and its application in system reliability prediction," Artificial Intelligence for Engineering Design, Analysis and Manufacturing, 33(3), pp.346-358.

[26] Hu, Z., and Du, X., 2019, "An exploratory study for predicting component reliability with new load conditions," Frontiers of Mechanical Engineering, 14(1), pp. 76-84.

[27] Yin, J., and Du, X., 2021, "A Safety Factor Method for Reliability-Based Component Design," Journal of Mechanical Design, 143(9), p. 091705.

[28] Rosenblatt, M., 1952, "Remarks on a multivariate transformation," The annals of mathematical statistics, 23(3), pp. 470-472.

[29] Huang, Z., and Jin, Y., 2009, "Extension of stress and strength interference theory for conceptual design-for-reliability," Journal of Mechanical Design, 131(7), p.071001.

[30] Sundararajan, C., and Witt, F., 1995, "Stress-strength interference method," Probabilistic Structural Mechanics Handbook, Springer, pp. 8-26.

[31] Liu, K., Wu, T., Detwiler, D., Panchal, J., and Tovar, A., 2019, "Design for crashworthiness of categorical multimaterial structures using cluster analysis and Bayesian optimization," Journal of Mechanical Design, 141(12), p.121701.

[32] Hu, Z., Mourelatos, Z. P., Gorsich, D., Jayakumar, P., and Majcher, M., 2020, "Testing Design Optimization for Uncertainty Reduction in Generating Off-Road Mobility Map Using a Bayesian Approach," Journal of Mechanical Design, 142(2), p.021402.

[33] Drezner, Z., 1994, "Computation of the trivariate normal integral," Mathematics of Computation, 62(205), pp. 289-294.

[34] Drezner, Z., and Wesolowsky, G. O., 1990, "On the computation of the bivariate normal integral," Journal of Statistical Computation and Simulation, 35(1-2), pp. 101-107.

[35] Genz, A., and Bretz, F., 1999, "Numerical computation of multivariate t-probabilities with application to power calculation of multiple contrasts," Journal of Statistical Computation and Simulation, 63(4), pp. 103-117.

[36] Wei, X., Han, D., and Du, X., 2021, "Approximation to multivariate normal integral and its application in time-dependent reliability analysis," Structural Safety, 88, p. 102008.

[37] Wu, H., and Du, X., 2020, "System Reliability Analysis With Second-Order Saddlepoint Approximation," ASCE-ASME Journal of Risk and Uncertainty in Engineering Systems, 6(4), p.041001.